AD-A057 355 NATIONAL BUREAU OF STANDARDS WASHINGTON D C F/G 11/9
PIEZOELECTRICITY AND PYROELECTRICITY IN POLYVINYLIDENE FLUORIDE--ETC(U)
JUL 78 M G BROADHURST, G T DAVIS N00014-78-C-0015
UNCLASSIFIED TR-9 NL

| OF |
AD
A057355

END
DATE
FILMED
9-78
DDC

(11) LEVEL II

OFFICE OF NAVAL RESEARCH

(15) Contract N00014-78-C-0015

Task No. NR 356-522

(9) Technical Report #9

(14) TR-9

(6) "Piezoelectricity and Pyroelectricity in Polyvinylidene Fluoride -- A Model"

by

(10) M.G. Broadhurst, G.T. Davis, J.E. McKinney and R.E. Collins

Prepared for Publication in

Journal of Applied Physics

National Bureau of Standards
Bulk Properties Section
Washington, D.C. 20234

(11) July 1978

(12) 27 p.

240 800

SECURITY CLASSIFICATION OF THIS PAGE (When Data Entered)

REPORT DOCUMENTATION PAGE

READ INSTRUCTIONS BEFORE COMPLETING FORM

1. REPORT NUMBER: Technical Report #9
2. GOVT ACCESSION NO.:
3. RECIPIENT'S CATALOG NUMBER:

4. TITLE (and Subtitle): "Piezoelectricity and Pyroelectricity in Polyvinylidene Fluoride -- A Model"

5. TYPE OF REPORT & PERIOD COVERED: Technical Report #9

6. PERFORMING ORG. REPORT NUMBER:

7. AUTHOR(s): M.G. Broadhurst, G.T. Davis, J.E. McKinney and R.E. Collins

8. CONTRACT OR GRANT NUMBER(s): N00014-78-C-0015

9. PERFORMING ORGANIZATION NAME AND ADDRESS:
National Bureau of Standards
Polymer Science and Standards Division
Washington, D.C. 20234

10. PROGRAM ELEMENT, PROJECT, TASK AREA & WORK UNIT NUMBERS: NR356-522

11. CONTROLLING OFFICE NAME AND ADDRESS:
Office of Naval Research
Chemistry Program
Arlington, VA 22217

12. REPORT DATE: July 1978

13. NUMBER OF PAGES: 26

14. MONITORING AGENCY NAME & ADDRESS (if different from Controlling Office):

15. SECURITY CLASS. (of this report): Unclassified

15a. DECLASSIFICATION/DOWNGRADING SCHEDULE:

16. DISTRIBUTION STATEMENT (of this Report)

According to attached distribution list.

DISTRIBUTION STATEMENT A
Approved for public release;
Distribution Unlimited

17. DISTRIBUTION STATEMENT (of the abstract entered in Block 20, if different from Report)

18. SUPPLEMENTARY NOTES

To be published in Journal of Applied Physics

19. KEY WORDS (Continue on reverse side if necessary and identify by block number)

Dipoles; piezoelectric; polarization; polymer; polyvinylidene fluoride; pyroelectric; space charge

20. ABSTRACT (Continue on reverse side if necessary and identify by block number)

A description is given of the molecular and morphological structure of polyvinylidene fluoride and from this description a classical model is proposed for calculating the piezo- and pyroelectric properties. The model consists of an array of crystal lamellae with a net moment from aligned dipoles in the crystals and compensating space charge on the crystal surfaces. The results for no compensation and complete compensation essentially bracket experimentally observed results and indicate that the largest contribution to the activity of this polymer arises from bulk dimensional changes, rather than from changes in molecular dipole moments.

DD FORM 1 JAN 73 1473 EDITION OF 1 NOV 65 IS OBSOLETE
S/N 0102-014-6601 |

SECURITY CLASSIFICATION OF THIS PAGE (When Data Ent...

Piezoelectricity and Pyroelectricity in Polyvinylidene Fluoride- A Model

by

M.G. Broadhurst, G.T.Davis, and J.E. McKinney
National Bureau of Standards
Washington, D.C. 20234

and
R. E. Collins
New South Wales Institute of Technology
Australia

Abstract

A description is given of the molecular and morphological structure of polyvinylidene fluoride and from this description a classical model is proposed for calculating the piezo- and pyroelectric properties. The model consists of an array of crystal lamellae with a net moment from aligned dipoles in the crystals and compensating space charge on the crystal surfaces. The results for no compensation and complete compensation essentially bracket experimentally observed results and indicate that the largest contribution to the activity of this polymer arises from bulk dimensional changes, rather than from changes in molecular dipole moments.

Piezoelectricity and Pyroelectricity in Polyvinylidene Fluoride- A Model*

by

M.G. Broadhurst, G.T. Davis, J.E. McKinney, and R.E. Collins

Introduction

Piezoelectric and pyroelectric properties of polyvinylidene fluoride (PVDF) and related semicrystalline polymers are receiving increasing attention as these polymers find use in transducer applications. There remains general uncertainty about the basic mechanism by which these effects occur. This paper considers some of the microscopic features of PVDF and calculates the electrical response expected from mechanical and thermal stresses.

A change in polarization (dipole moment per unit volume) can occur through changes in either the moment or the volume. An organic substance, such as PVDF, has large (relative to inorganic and metallic materials) compressibility and thermal expansion coefficients, and with aligned dipoles present, can yield large polarization changes through changes in volume[1,2] (sometimes referred to as secondary piezoelectricity)[3]. Most proposed mechanisms for activity in PVDF focus on changes in the moment. Aslaksen[4] considered effects of thermally induced orientational fluctuations in PVDF dipoles. Ohigashi[5] proposed increased dipole alignment when a PVDF molecule is mechanically stressed. Date[6] and Wada and Hayakawa[7] have considered a model with polar spheres dispersed in a non-polar

*Work supported in part by the Office Of Naval Research.

medium. The importance of trapped space charge has been proposed by several authors[8-10]. Hayakawa and Wada[7] have examined the contribution of trapped charge where there are mechanical heterogenieties present, and Crosmier et.al.[11] have shown that trapped charge does lead to measureable piezoelectric activity. Hayakawa and Wada have considered several mechanisms in a recent review article[7] and Oshiki and Fukada[12] have considered electrostriction effects.

So far, models for piezoelectricity and pyroelectricity are fragmentary. This paper pulls together available information on the microscopic structure of PVDF in order to make a relatively complete but simple and realistic model. The response of the model is calculated from physically measureable parameters and the results compared to published data. The calculated response contains contributions from dimensional changes, dipole orientational fluctuations, electrostriction and space charge and accounts for most of the observed response.

Microscopic Details of PVDF

PVDF crystallizes from the melt into spherulitic structures[13]. Figure 1 is a photomicrograph of a melt-crystallized PVDF film taken between crossed polaroids. The volume fraction of crystalline material is typically about 50% depending on thermal history[14]. Most of the uncrystallized molecules are in a metastable supercooled liquid phase. The glass transition temperature for this liquid phase is around -50°C from volume[15] and dielectric data[16,17,18]. Based on similarities in molecular structure and phase behavior between PVDF and the much more widely studied polyethylene[19] we can assume similar spherulitic structures, as shown in Fig. 2. That is, the spherulites consist of stacks of lamellae which grow outward from the center of the spherulite. These lamellae are typically 10 to 20 nm thick[14],

again depending on crystallization conditions. The molecular chains are approximately normal to the large lamellae surfaces and to the radii of the spherulites[19]. Much of the liquid material is probably located between the crystalline lamellae. That is, a typical region (Fig. 2) consists of parallel layers of alternating crystal and liquid material each layer of the order of 10 to 20 nm thick. Of course, on a larger scale one expects the usual stacking faults, grain boundaries and other course defects typically found in a polycrystalline solid. Since the molecular lengths are of the order of 100 times the lamellae thickness, each molecule must pass many times through one or more of the crystal and liquid layers, being confined to elongated linear segments in the crystal layers and free to assume flexible and irregular configurations in the liquid layers.

PVDF is inherently polar (Fig. 3). The hydrogen atoms are positively charged and the fluorine atoms negatively charged with respect to the carbon atoms in the polymer. The net moment of a group of molecules in a liquid region of PVDF will be zero in the absence of an applied field because of the random orientation of individual dipoles. In the crystal, however, there are two crystal phases, β and γ (forms I and III) where the molecules are reported to form a planar zig-zag conformation[20] with the dipole moments parallel in the unit cell (Fig. 4). β and γ crystal forms of PVDF are therefore inherently polar and a given crystal lamella will have a net polarization equal to that of a single repeat unit (ignoring defects for the time being). Since the dipole moment will be normal to the molecular axis, the crystal polarization will also be normal to the molecular axis and hence approximately parallel to the plane of the lamellae.

A third crystal form, α (Form II), has a net dipole moment with a component normal to the molecular axis but the chains pack to form an antipolar unit cell[20] and hence non-polar lamellae. Such a crystal would not be applicable to the present model unless it could be given a stable polarization by virtue of an electric field-induced crystal modification to a polar form. Activity in the α phase has been reported[5,21] and some evidence for a field-induced polar modification of the normally antipolar α phase has been given[22,24]. However, few structural details are available at present.

Molecular Moment of a PVDF Crystal

If a crystal consists of molecular repeat units having a vacuum moment μ_o, then the reaction field from any medium surrounding μ_o will further polarize the molecule and enhance its moment. If we assume an isotropic, low-field crystal permittivity of ε_c, then continuum theory predicts[25] that the electric field external to μ_o but still within the crystal will be equal to that from a dipole of moment

$$m = \frac{\varepsilon_c + 2}{3} \mu_o \qquad (1)$$

Near the surface of the crystal the dipole is exposed to material of a different permittivity. To minimize the resultant surface effects, the crystals must be large.

All the n dipoles in a particular crystal have the same mean orientation, and fluctuate about this mean because of thermal energy. Thus, the moment of the crystal due to dipole alignment, m_d, will be

$$m_d = n \frac{\varepsilon_c + 2}{3} \mu_o \langle \cos \phi \rangle u, \qquad (2)$$

where ϕ is the angle between the mean and instantaneous orientations of a dipole and u is a unit vector in the direction of m_d.

This crystal moment due to dipole alignment creates electric fields in the surrounding material, and because of the finite conductivity of PVDF, produces free charge motion. The effect of the free charges on the moment of the crystal must be considered.

As with most highly polar organic materials, the conductivity (or equivalently the dielectric loss) of PVDF depends on ionic impurity concentration, which in turn depends on sample history[26,27] and field strength[28]. Typically the resistivity, ρ is 10^{14} to 10^{15} Ω cm for PVDF at room temperature, and the relative permittivity $\varepsilon_s/\varepsilon_o$ is 10 to 15.[18] The Maxwell relaxation time, (the relaxation time for a non-equilibrium distribution of charge in the material), $\tau_m = \rho\ \varepsilon_s$, will be of the order of minutes to hours near room temperature. If any polar crystal of PVDF is located within the conducting sample we expect its dipolar surface charge to be at least partially neutrallized by ionic charges within the time the sample is usually stored before use. The degree of charge compensation will depend on the number of charge carriers available. This compensation of dipole charges by free charges is similar to the interfacial polarization often observed in two phase dielectrics. Free charge compensation of dipole polarization has been observed in the bulk of a polymer which has been non-uniformly polarized[29] but has yet to be demonstrated at the crystal-liquid interface.

For times short compared to the Maxwell relaxation time we can write the moment due to free charges at the crystal-liquid interface as

$$\underline{m}_q = q\ \ell_c\ \underline{u}, \tag{3}$$

where q is a constant amount of charge, and ℓ_c is the mean separation of the negative and positive charges on a crystal. We take this to be the mean crystal length in the direction of u.

The total moment of the crystal with it's countercharge at or near equilibrium is

$$m_c = m_d + m_q = [n(\varepsilon_c + 2)\, \mu_o \langle \cos \phi \rangle / 3 + q\, \ell_c]\, u. \qquad (4)$$

Because of the relaxation time required for q to change, even if m_c is initially zero, a perturbation of the sample by thermal or mechanical stress will affect m_d and m_q differently and produce a net moment.

Effect of Crystal Polarization on Sample Polarization

Changes in m_c will be coupled to the electrodes through the surrounding semicrystalline material which acts, in the simplist view, as an RC coupling network. The apparent moment m_s, external to the crystal, will depend on the shape, size, orientation, and permittivity of the crystal and the permittivity and conductivity of the sample and on time. That is

$$m_s = f\, m_c \qquad (5)$$

where f can be calculated for simple crystal geometries only. One convenient choice is to assume a spherical crystal particle of permittivity ε_c in which case, according to continuum theory,[25] the apparent moment external to the crystal will be

$$m_s = \frac{3\varepsilon_s}{2\varepsilon_s + \varepsilon_c}\, m_c \text{ (spherical crystals)} \qquad (6)$$

where ε_s is the permittivity of the composite sample surrounding a given crystal.

This result is for times short compared to the Maxwell relaxation time and corresponds to the result given previously for this model.[7] We have obtained a numerically similar result for the case of spherical liquid particles dispersed in the crystal phase.

More realistic than either spherical crystal or liquid particles, in the light of the earlier discussion of the morphology of semicrystalline polymers, is a model where the crystals are thin lamellae with the polarization in the plane of the lamellae (Fig. 5). In this case very little of the field due to the crystal moment is internal to the particle and

$$m_s = m_c \text{ (lamellar crystals)} \tag{7}$$

which is rigorously true for infinitely thin crystals, and a much better approximation for the case at hand than Eq.(6).

In practice, piezoelectric polymers are usually in the form of thin films and the stress-induced moment is measured normal (z axis in Fig. 5) to the plane of the film. From Eq.(4) this component of the sample moment is

$$m_s = (m_d \langle \cos \theta \rangle + m_q \cos \theta_o) \tag{8}$$

where θ is the angle from the z axis to an individual dipole at any instant in time, θ_o is the time average of θ, and $\langle \cos \theta \rangle$ is the average over all dipoles in the crystal. The projection of m_d involves the projection of each (librating) dipole moment prior to averaging and that of m_q involves only the net moment.

Using the classical harmonic oscillator approximation for dipole fluctuations it has been shown that[2]

$$\langle \cos \theta \rangle = \cos \theta_o \, J_o(\phi_o) \tag{9}$$

where ϕ_o is the average amplitude of librations for a dipole about the extended molecular axis and $J_o(\phi_o)$ is the zeroth order Bessel function of the first kind.

Thus,

$$m_s = [n(\varepsilon_c + 2)\,\mu_o J_o(\phi_o)/3 + q\,\ell_c]\cos\theta_o \tag{10}$$

Total Moment for a Dispersion of Lamellar Crystals

If one extends the above single crystal result (10) to a film sample containing a dispersion of lamellar crystals of the same kind but varying in number of dipoles, n, mean orientation, θ_o, and countercharge, q, then we can write the moment for the entire sample as

$$M_s = \Sigma\, m_s = [N(\varepsilon_c + 2)\mu_o J_o(\phi_o)/3 + \mathcal{Q}\,\ell_c]\,\langle\cos\theta_o\rangle \tag{11}$$

where for a large number of crystals containing a total of N dipoles, $N = \Sigma n$ over all crystals, $\mathcal{Q} = \Sigma q$ over all crystals and

$$\langle\cos\theta_o\rangle = \int_o^{\pi} n(\theta_o)\cos\theta_o\, d\theta_o \Big/ \int_o^{\pi} n(\theta_o)\, d\theta_o \tag{12}$$

is the average $\cos\theta_o$, and $n(\theta_o)$ is the number of dipoles having an orientation between θ_o and $\theta_o + d\theta_o$.

The charge per unit electrode area A_s induced by M_s on electrodes in intimate contact with a sample film of PVDF is given by

$$Q_s/A_s = M_s/\ell_s A_s \equiv P_s \tag{13}$$

where ℓ_s is the thickness and P_s is the total polarization of the sample. Thus the charge on the electrodes induced by M_s is

$$Q_s = [N(\varepsilon_c + 2)\mu_o J_o(\phi_o)/3 + \mathcal{Q}\,\ell_c]\,\langle\cos\theta_o\rangle/\ell_s \tag{14}$$

Calculation of the Piezoelectric and Pyroelectric Coefficients

Although rigorously speaking the piezoelectric and pyroelectric coefficients are defined as derivatives of the electric displacement (or equivalently the polarization under short circuit conditions), in practice one usually adopts the definitions,

$$d_p \equiv A^{-1}\, dQ_s/dp \tag{15a}$$

for the hydrostatic piezoelectric coefficient, and

$$p_y \equiv A^{-1}\, dQ_s/dT \tag{15b}$$

for the pyroelectric coefficient, where p and T are the pressure and temperature respectively. These definitions give the commonly measured quantities. To calculate these for the present model we merely take derivatives of Eq.(14) using the relationships given in more detail previously.

$$\begin{aligned}
\partial\varepsilon_c/\partial X &= -(\varepsilon_c - 1)(\varepsilon_c + 2)\,[\partial(\ln v_c)/\partial X]/3 \\
\partial J_o(\phi_o)/\partial X &= -J_1(\phi_o)\,\partial\phi_o/\partial X \\
\partial\phi_o/\partial p &= \phi_o\,\gamma\,\partial(\ln v_c/\partial p) \\
\partial\phi_o/\partial T &= \phi_o/2T + \phi_o\,\gamma\,\partial(\ln v_c)/\partial T \\
\partial\ell_c/\partial X &= [\partial(\ln \ell_c)/\partial(\ln v_c)]\partial(\ln v_c)/\partial X \\
\partial\ell_s/\partial X &= [\partial(\ln \ell_s)/\partial(\ln v_c)]\partial(\ln v_c)/\partial X
\end{aligned} \tag{16}$$

where X equals either temperature, T, or pressure, p, v_c is the crystal volume, $\partial(\ln v_c)/\partial T$ is the thermal coefficient of volume expansion, α_c, and $\partial(\ln v_c)/\partial p$ the volume compressibility, β_c, $J_1(\phi_o)$ is a first order Bessel function of the

first kind, and $\gamma = \partial(\ln \omega)/\partial(\ln v_c)$ is the Gruneisen coefficient for dipole librational frequency ω. In the above, partial derivatives with respect to T are at constant p and those with respect to p are at constant T. To simplify the calculation we assume the number of dipoles, N, their vacuum moment, μ_o, and the countercharge, $\mathcal{Q}$, and the crystal orientations, $\cos \theta_o$ do not change with pressure and temperature, and we consider changes in the obvious variables, ε_c, J_o, ℓ_c and ℓ_s only.

For the case of no countercharge at the crystal liquid interface,

$$d_p = P_o \beta_c[(\varepsilon_c - 1)/3 + \phi_o^2 \gamma/2 + \partial(\ln \ell_s)/\partial \ln v_c] \tag{17a}$$

$$p_y = - P_o \alpha_c[(\varepsilon_c - 1)/3 + \phi_o^2(\gamma + (2T\alpha_c)^{-1})/2 + \partial(\ln \ell_s)/\partial(\ln v_c)] \tag{17b}$$

and for the case of complete neutralization of dipole charge by countercharge at the crystal-liquid interfaces

$$d_p = P_o \beta_c[(\varepsilon_c - 1)/3 + \phi_o^2 \gamma/2 + \partial(\ln \ell_c)/\partial \ln v_c)] \tag{18a}$$

$$p_y = - P_o \alpha_c[(\varepsilon_c - 1)/3 + \phi_o^2(\gamma + (2T\alpha_c)^{-1})/2 + \partial(\ln \ell_c)/\partial(\ln v_c)] \tag{18b}$$

In both cases above,

$$P_o = \Phi(\varepsilon_c + 2)\, N \mu_o J_o(\phi_o) \langle \cos \theta_o \rangle / 3V_c \tag{19}$$

where $\Phi = V_c/V_s$ is the volume fraction of crystals, N/V_c the number of dipoles per unit crystal volume, and for small values of ϕ_o,

$$\phi_o^2/2 \approx \phi_o J_1(\phi_o)/J_o(\phi_o) \tag{20}$$

Note that the only distinction between the above equations for no and full countercharge is that ℓ_s appearing in eqs.(17) becomes ℓ_c in the corresponding eqs.(18).

Comparison with Experiment

Eqs.(17) and (18) can be evaluated using reasonable values for the experimental quantities as listed in Table I. The α_c[30] and β_c[31] are from x-ray data on α phase PVDF. These values should be a little less for the slightly denser β phase of interest here.

The partial derivatives of the crystal length ℓ_c, in the crystal polarization direction (b axis in the β phase) are taken as $\alpha_c/2$ and $\beta_c/2$ based on negligible expansion along the molecular axis[32] (c axis in the β phase). The partial derivatives of the sample thickness, ℓ_s, are also taken as 1/2 the corresponding bulk sample expansion coefficient, $\alpha_s/2$ and compressibility, $\beta_s/2$.

The Gruneisen parameter γ giving the volume dependence of the librational frequencies should be an average over all librational mode frequencies each weighted according to it's corresponding librational amplitude. It is estimated here to be that typically computed from the modulus for linear polymers.[32] The rms librational amplitude is estimated from data on polyethylene[33] and is close to the value found for (CH_2-CHCl) dipoles in polyvinylchloride below the glass transition temperature.[2] The room temperature ε_c is estimated from low temperature dielectric data where the reorientational contribution from the liquid is absent. P_o can be measured directly[23,24], and its maximum value can be estimated from Eq.(19). The orientation function $\langle\cos\theta_o\rangle$, however, is not measureable directly by known techniques. Both NMR and IR measurements yield $\langle\cos^2\theta_o\rangle$ and x-ray data cannot distinguish between two crystals if one is rotated by π radians with respect to the other. Kepler[34] analyzed x-ray data

on polarized PVDF by assuming a distribution function, $n(\theta_o) = \exp(aF \cos \theta_o)$, where F is the polarizing electric field. In the general case, however, we are unable to calculate P_o in Eq.(17c), and must use measured values of P_o to calculate d_p and p_y. Fortunately one can measure P_o by measuring the charge needed to polarize a specimen[23,24] or by measuring the charge released while the specimen is heated above its crystal melting temperature[35]. The experimental values used to check the theory are shown in Table 1. Table II gives calculated and experimental quantities and shows the contribution due to various sources.

Sources of Uncertainty

Table II summarizes the predicted contributions from Eqs.(17) and (18) using the values from Table I. The calculation of d_p/P_o and p_y/P_o are probably no better than 20% due to uncertainty in experimental values used. The agreement with experiment is better for the case of very little countercharge. The question of the extent of countercharge depends on the concentration of charge carriers present which is not known at present. The assumption that the charge, $\mathcal{Z}$, remains constant seems reasonable in the light of our discussion of the Maxwell time constant and the absence of observed time effects with PVDF. If the dipole moment, μ_o, changed, one would expect it to get smaller with pressure and larger with temperature, which is opposite the other contributions.

Kepler and Anderson[36] have proposed that reversible temperature dependent crystallinity is responsible for much of the pyroelectricity in PVDF. One might suppose that N changes by virtue of such a reversible pressure and temperature dependent crystallization of dipole units. That is, if the pressure is increased or the temperature decreased there could be a slight increase in the number of

repeat units associated with the crystal. A significant contribution to the response could occur if only one in every 10^4 repeat units crystallized or melted per degree or per 10^6 N/m^2 (10 atmospheres) change in temperature or pressure. So small a change is difficult to measure by other techniques and this possibility remains speculative.

The temperature and pressure dependences of d_p and p_y can be found by taking derivatives of Eqs. (17) and (18). These derivatives are cumbersome and hard-to-measure quantities (eg. γ and ℓ_c). Thus it is simpler to evaluate d_p and p_y at various temperatures and pressures by using the required measured quantities determined at those same temperatures and pressures. In the glass transition region near - 40^oC the change in sample and crystal volumes, for example, will be especially dependent on temperature and pressure. Fractional changes in p_y of about $10^{-2}K^{-1}$ are generally reported at room temperature [39,40] and a more careful evaluation of the experimental quantities in Eqs. (17) and (18) as functions of temperature and pressure is underway[41].

The difference in activity between β phase and postulated polar α phase material will probably not be large. On the one hand, the dipole moment per monomer perpendicular to the molecular chain is smaller for the α phase ($4x10^{-2}$ Ccm versus $7x10^{-28}$ Ccm for the β phase). Compensating for this are an increased expansion coefficient and compressibility for the α phase[41].

The dependence of d_p and p_y on poling conditions is, by the present model, due solely to the dependence of P_o (Eq(19)) on poling conditions. In the present paper we calculate d_p and p_y for any value (measured) of P_o. The dependence of P_o on the distribution of local electric fields in the sample, the duration and temperature at which the poling voltage is applied and the ionic impurity concentration and metal electrode-
[illegible] which affect the local fields will be considered in [illegible]

At present, it seems there is little if any of the observed activity in PVDF which cannot be accounted for by the simple classical mechanisms in the present model. The model predicts that the ratio of piezoelectric to pyroelectric response will be about 50 K cm^2N^{-1} in good agreement with experiment.

Implications for Applications

The maximum polarization from Eq.(19) is 20 $\mu C/cm^2$ including the reaction field contribution. Assuming the model is correct commonly produced oriented films of PVDF have about 1/3 the maximum polarization[23,24,35] and activity obtainable with a single crystal. The activity could be increased either by increasing the crystal fraction or by orienting the existing crystals better, though it seems unlikely that presently achievable activity can be doubled without destroying mechanical strength of the film. Also, minimizing countercharge by limiting charge carrier concentration maximizes activity as seen in Table II. If countercharge is present, it is possible that an increase in the conductivity by the addition of ions can improve the coupling between crystal and electrodes (resistive coupling rather than the capacitive coupling used in this paper). We have not succeeded in calculating the possible enhancement from a highly conductive sample, except in the case of non-uniformly polarized specimens.

Table I

Experimental Values

Quantity	Value	Reference
T	300 K	-
α_c	$1.7 \times 10^{-4} k^{-1}$	30
β_c	$1.1 \times 10^{-10} Nm^{-2}$	31
α_s	$4.2 \times 10^{-4} k^{-1}$	30
β_s	$2.39 \times 10^{-10} Nm^{-2}$	36, 37
ε_c	3	32, 18
γ	5	18, 32
ϕ_o	16°	33
Φ	0.5	14
$N\mu_o/V_c$*	$12 \times 10^{-6} C\ cm^{-2}$	38
d_p/P_o	$2 \times 10^{-6}\ cm^2 N^{-1}$	24
p_y/P_o	$4 \times 10^{-4}\ K^{-1}$	23,24

*β phase with 5% head-head defects in molecule.

Table II

Calculated Contributions to Piezoelectricity and Pyroelectricity in PVDF

Source of Response	d_p/P_o ($\times 10^{-6}$ cm^2N^{-1}) value	(% of exp. total)	p_y/P_o ($\times 10^{-4}$ K^{-1}) value	(% of exp. total)
Electrostriction	0.74	(37)	1.14	(28)
Dipole Fluctuations	0.21	(10)	0.98	(24)
Dimensional Changes in				
ℓ_c (with countercharge)	0.55	(28)	0.85	(21)
ℓ_s (without countercharge)	1.2	(60)	2.1	(52)
Total Calculated Response				
(with countercharge)	1.50	(75)	2.97	(74)
(without countercharge)	2.15	(107)	4.22	(106)

References

1. E. P. Adams, J. Franklin Inst., 204, 469 (1927).
2. F. I. Mopsik and M. G. Broadhurst, J. Appl. Phys., 46, 4204 (1975).
3. W. G. Cady, Piezoelectricity, McGraw Hill, New York, N.Y. (1946) p.701.
4. E. W. Aslaksen, J. Chem. Phys., 57, 2358 (1972).
5. H. Ohigashi, J. Appl. Phys., 47, 949 (1976).
6. M. Date, Polymer J., 8, 60 (1976).
7. Y. Wada and R. Hayakawa, Japan. J. Appl. Phys., 15, 2041 (1976).
8. G. Pfister, M. Abkowitz, and R. G. Crystal, J. Appl. Phys., 44, 2064 (1973).
9. N. Murayama, T. Oikawa, T. Katto, and K. Nakamura, J. Polym. Sci., Polym. Phys. Ed., 13, 1033 (1975).
10. S. Hunklinger, H. Sussner and K. Dransfeld, Festkorperprobleme XVI, 267 (1976).
11. J. J. Crosnier, F. Micheron, G. Dreyfus, and J. Lewiner, J. Appl. Phys, 47, 4798 (1976).
12. M. Oshiki and E. Fukada, J. Mat'l. Sci., 10, 1 (1975).
13. W. M. Prest, Jr. and D. J. Luca, J. Appl. Phys., 46, 4136 (1975).
14. K. Nakagawa and Y. Ishida, J. Polym. Sci., Polym. Phys. Ed., 11, 2153 (1973).
15. L. Mandelkern, G. M. Martin and F. A. Quinn, Jr., J. Res. Nat. Bur. Stds. (USA) 58, 137 (1957).
16. H. Sasabe, S. Saito, M. Asahina, and H. Kakutani, J. Polym. Sci., A-2, 7, 1405 (1969).
17. M. Abkowitz and G. Pfister, J. Appl. Phys., 46, 2559 (1975).
18. H. Kakutani, J. Polym. Sci., A-2, 8, 1177 (1970).
19. F. Khoury and E. Passaglia, The Morphology of Crystalline Synthetic Polymers in "Treatise on Solid State Chemistry Vol.3 (Plenum Press, N.Y. 1976) N. B. Hannay, ed. Chap. 6, p.445.
20. R. Hasegawa, Y. Takahashi, Y. Chatani and H. Tadokoro, Polymer J., 3, 600 (1972).

21. G. R. Davies, A. Killey, A. Rushworth, and H. Singh, Organic Coatings and Plastics Chemistry, 38, 257 (1978) (Preprints for ACS Meeting in Anaheim, CA, March 1978.)

22. J. P. Luongo, J. Polymer Sci., A-2, 10, 1119 (1972).

23. P. D. Southgate, Appl. Phys. Letters, 28, 250 (1976).

24. J. E. McKinney and G. T. Davis, Organic Coatings and Plastics Chemistry, 38, 271 (1978) (Preprints for ACS Meeting in Anaheim, CA, March 1978.)

25. H. Frohlich, "Theory of Dielectrics" (Oxford University Press, London 1950) p.16.

26. S. Osaki, S. Uemura, and Y. Ishida, J. Polymer Sci., A-2, 9, 585 (1971).

27. S. Uemura, J. Polymer Sci. Polymer Phys. Ed., 10, 2155 (1972).

28. H. Sussner and D. Y. Yoon, Organic Coatings and Plastics Chemistry, 38, 331 (1978) (Preprints for ACS Meeting in Anaheim, CA, March 1978.)

29. M. G. Broadhurst, G. T. Davis, S. C. Roth, and R. E. Collins, Proceedings of Conference on Electrical Insulation and Dielectric Phenomena, Buck Hill Falls, Pa. October 1976.

30. K. N. Nakagawa and Y. I. Ishida, Kolloid Z.Z. Polymere, 251, 103 (1973).

31. B. A. Newman, C. H. Yoon, and K. D. Pae, Technical Report No. 11 under Office of Naval Research Contract N00014-75-C-0540.

32. M. G. Broadhurst and F. I. Mopsik, J. Chem. Phys., 52, 3634 (1970).

33. K. Iohura, K. Imada, and M. Takayanagi, Polymer J., 3, 357 (1972).

34. R. G. Kepler and R. A. Anderson, to be published in J. Appl. Phys. (1978).

35. R. G. Kepler, Organic Coatins and Plastics Chemistry, 38, 278 (1978) (Preprints for ACS Meeting in Anaheim, CA, March 1978.)

36. R. G. Kepler and R. A. Anderson, to be published in J. Appl. Phys. (1978).

37. W. W. Doll and J. B. Lando, J. Macromol. Sci. Phys., B2, 219 (1968).

38. G. T. Davis in "Proceedings of Piezoelectric and Pyroelectric Symposium-Workshop" NBSIR 75-760, p.120.

39. W. R. Blevin, Appl. Phys. Letters 31, 6 (1977).

40. H. Burkard and G. Pfister, J. Appl. Phys. 45, 3360 (1974).

41. B. A. Newman, Rutgers University private communication.

Figure Captions

FIGURE 1 Photomicrograph of a rapidly cooled melt of commercial unoriented PVDF between crossed polaroids.

FIGURE 2 A schematic diagram of a spherulite and a detail of a section emphasizing the lamellar structure of the radiating branches.

FIGURE 3 A model of two configurations of a PVDF molecular segment. The small black balls represent carbon atoms, the large ones represent fluorine atoms and the white tips, hydrogen atoms. Note both forms have a net dipole moment normal to the long axis.

FIGURE 4 A schematic diagram of the unit cells as viewed along the chain direction (a b projection) normally crystallized from the two configurations of Figure 3. Forms I and III (β and γ) are polar and Form II (α) is antipolar.

FIGURE 5 A schematic diagram showing dipole alignment and counter-charge on a lamellar section of polar crystal. In this paper we calculate the response from a preferentially aligned array of such objects in a semicrystalline sample.

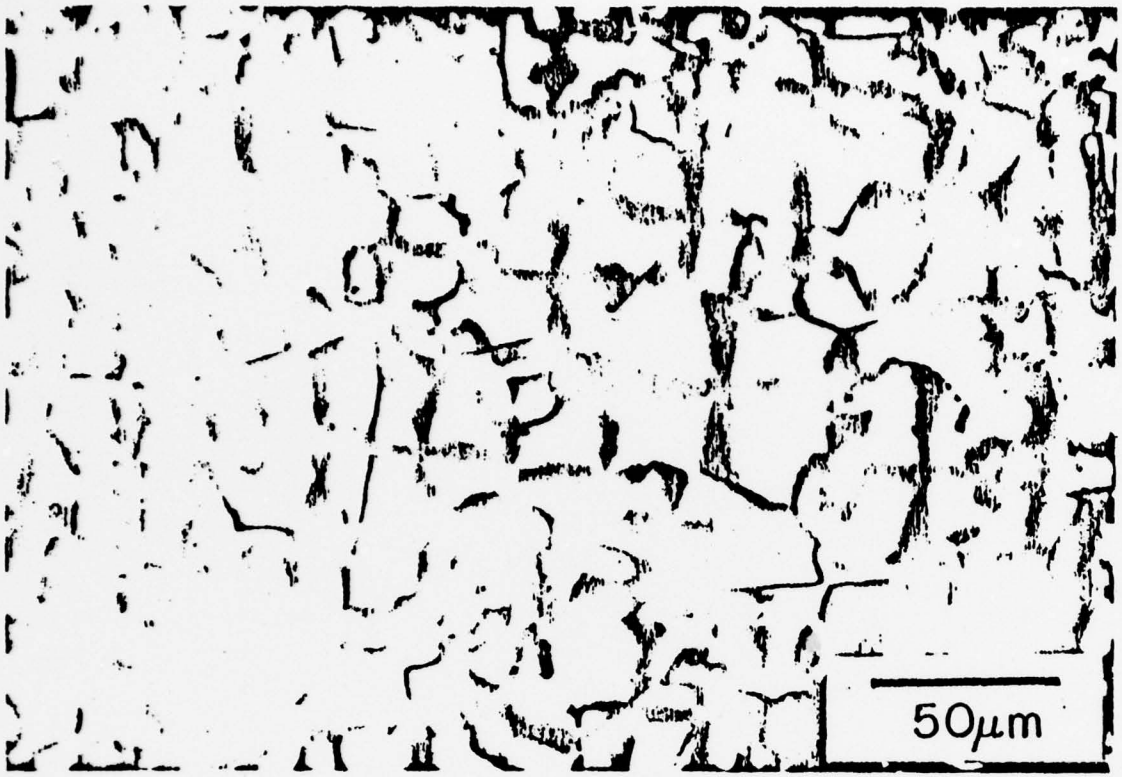
50μm

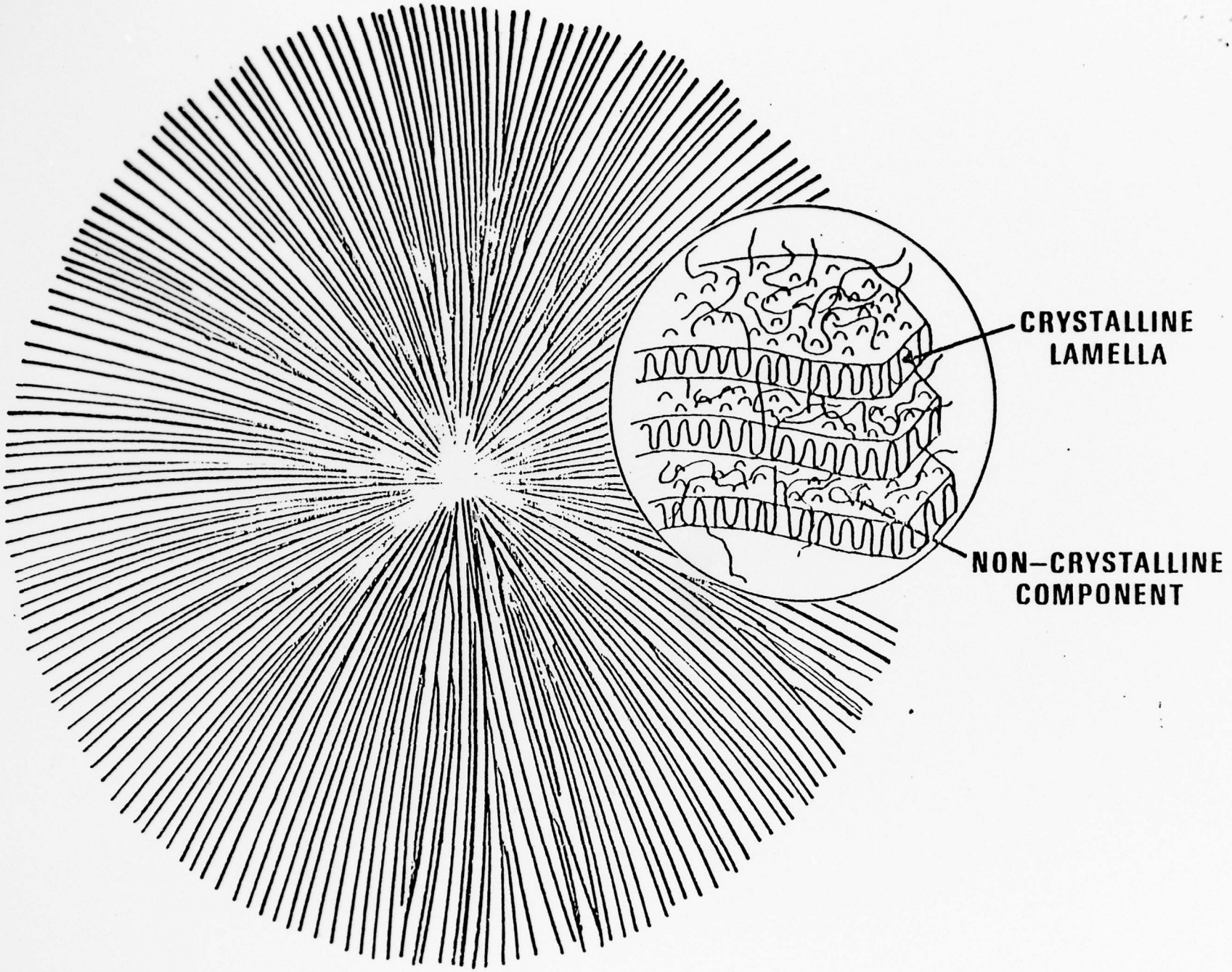
CRYSTALLINE
LAMELLA
NON–CRYSTALLINE
COMPONENT

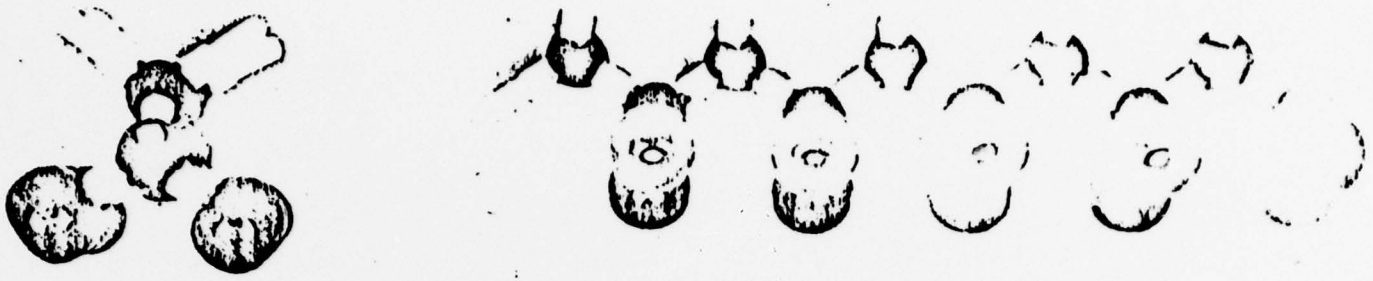

I, β; III, γ

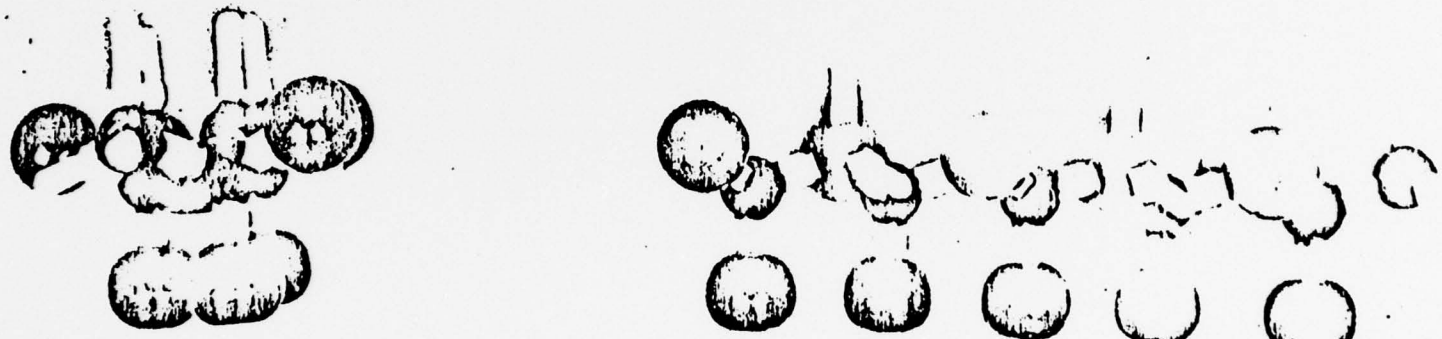

II, α

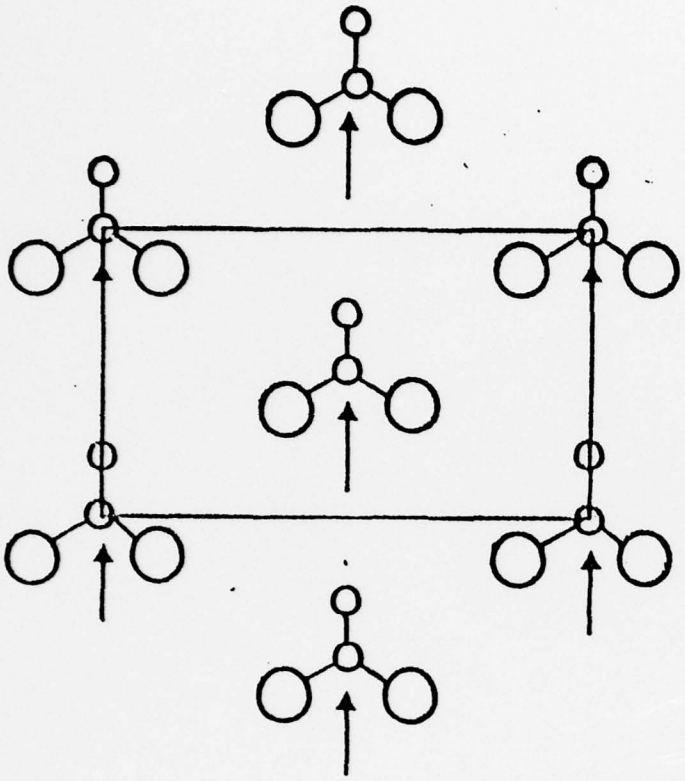

FORMS I and III

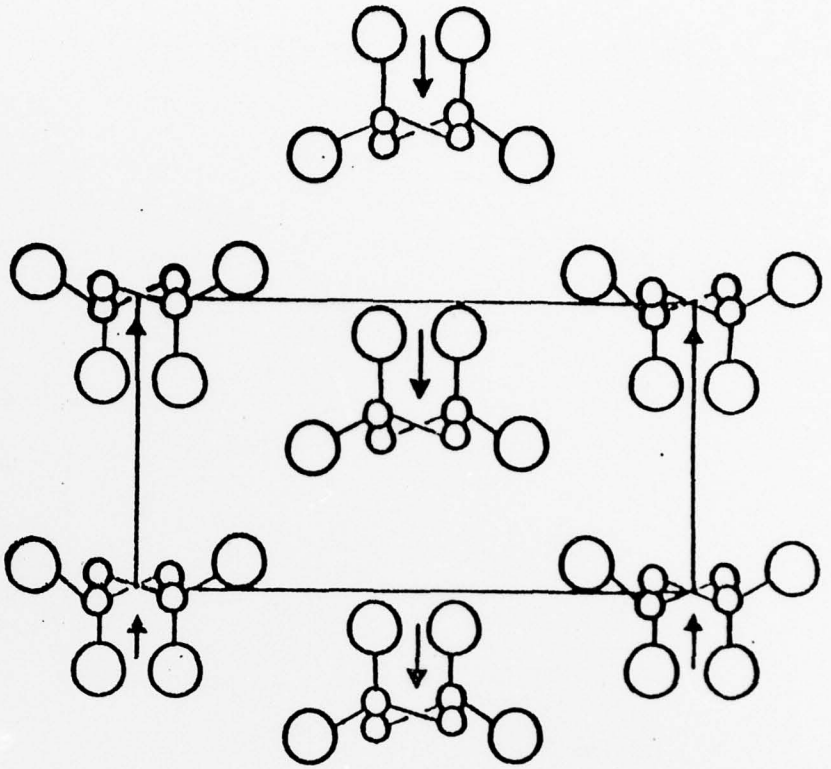

FORM II

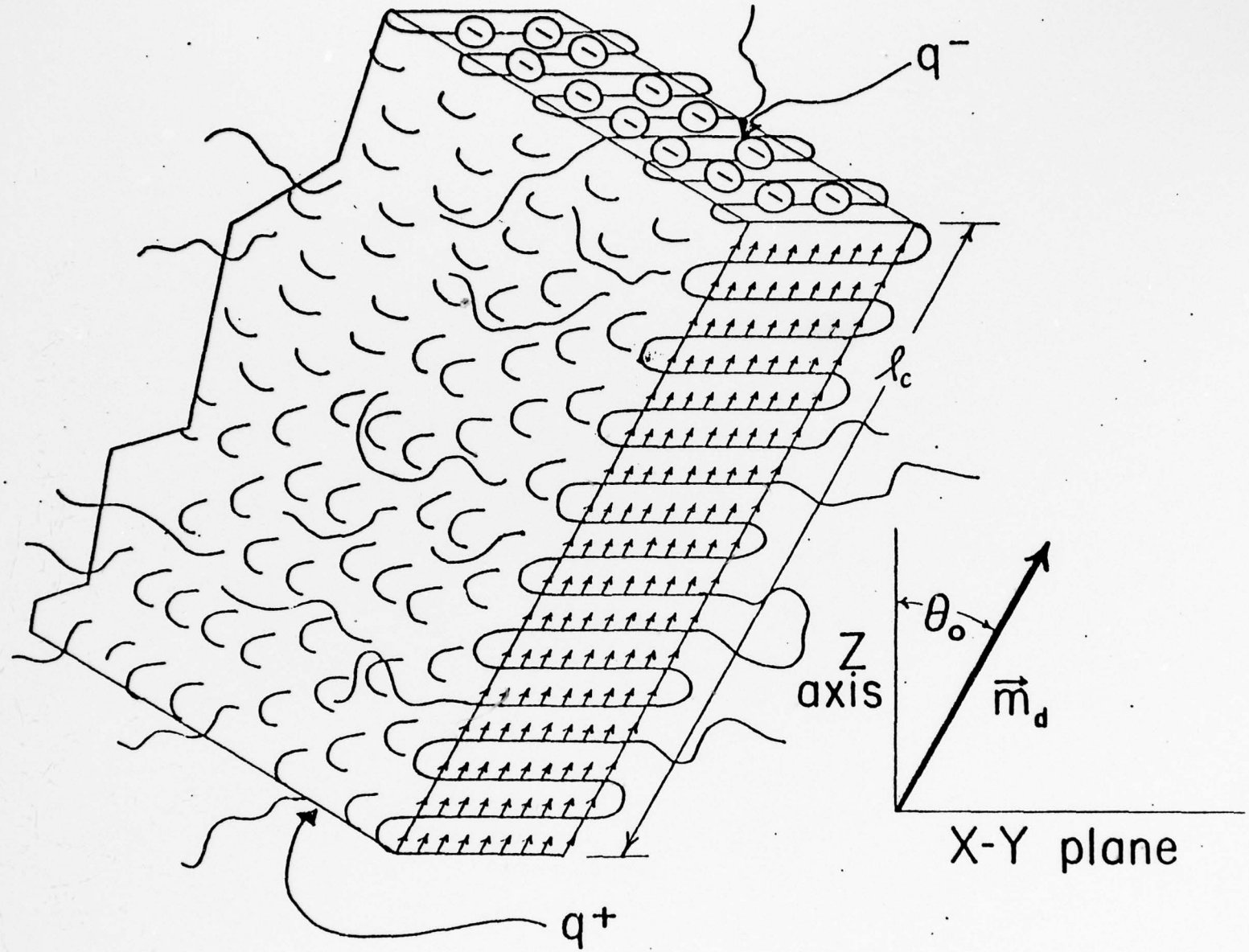
FILM SURFACE
q⁻
ℓ_c
θ_o
Z axis
$\vec{m}_d$
X-Y plane
q+

TECHNICAL REPORT DISTRIBUTION LIST

	No. Copies
Dr. Stephen H. Carr Department of Materials Science Northwestern University Evanston, Illinois 60201	1
Dr. M. Broadhurst Bulk Properties Section National Bureau of Standards U.S. Department of Commerce Washington, D.C. 20234	2
Dr. C. H. Wang Department of Chemistry University of Utah Salt Lake City, Utah 84112	1
Dr. T. A. Litovitz Department of Physics Catholic University of America Washington, D.C. 20017	1
Dr. R. V. Submaranian Washington State University Department of Materials Science Pullman, Washington 99103	1
Dr. M. Shen Department of Chemical Engineering University of California Berkeley, California 94720	1
Dr. R. S. Porter Polymer Research Institute and Polymer Science and Engineering University of Massachusetts Amherst, Massachusetts 01002	1
Dr. Morton Litt Dept. of Macromolecular Science Case Western Reserve University Cleveland, Ohio 44106	1
Dr. V. Stannett Department of Chemical Engineering North Carolina State University Raleigh, North Carolina 27607	1
Dr. D. R. Uhlman Department of Metallurgy and Material Science Center for Materials Science and Engineering Massachusetts Institute of Technology Cambridge, Massachusetts 02139	1
Naval Surface Weapons Center White Oak Silver Spring, Maryland 20910 Attn: Dr. J. M. Augl Dr. B. Hartmann	1
Dr. G. Goodman Globe Union Inc. 5757 North Green Bay Avenue Milwaukee, Wisconsin 53201	1
Picatinny Arsenal SMUPA-FR-M-D Dover, New Jersey 07801 Attn: A. M. Anzalone Bldg. 3401	1
Dr. J. K. Gillham Princeton University Department of Chemistry Princeton, New Jersey 08540	1
Douglas Aircraft Co. 3855 Lakewood Boulevard Long Beech, California 90846 Attn: Technical Library Cl 290/36-84 AUTO-Sutton	1
Dr. E. Baer Department of Macromolecular Science Case Western Reserve University Cleveland, Ohio 44106	1
Dr. K. D. Pae Department of Mechanics and Materials Science Rutgers University New Brunswick, New Jersey 08903	1

TECHNICAL REPORT DISTRIBUTION LIST

	No. Copies
Office of Naval Research Arlington, Virginia 22217 Attn: Code 472	2
Office of Naval Research Arlington, Virginia 22217 Attn: Code 102IP	6
ONR Branch Office 536 S. Clark Street Chicago, Illinois 60605 Attn: Dr. George Sandoz	1
ONR Branch Office 715 Broadway New York, New York 10003 Attn: Scientific Dept.	1
ONR Branch Office 1030 East Green Street Pasadena, California 91106 Attn: Dr. R. J. Marcus	1
ONR Branch Office 760 Market Street, Rm. 447 San Francisco, California 94102 Attn: Dr. P. A. Miller	1
ONR Branch Office 495 Summer Street Boston, Massachusetts 02210 Attn: Dr. L. H. Peebles	1
Director, Naval Research Laboratory Washington, D.C. 20390 Attn: Library, Code 2029 (ONRL) Technical Info. Div. Code 6100, 6170	6 1 1
The Asst. Secretary of the Navy (R&D) Department of the Navy Room 4E736, Pentagon Washington, D.C. 20350	1
Commander, Naval Air Systems Command Department of the Navy Washington, D.C. 20360 Attn: Code 310C (H. Rosenwasser)	1

	No. Copies
Defense Documentation Center Building 5, Cameron Station Alexandria, Virginia 22314	12
U.S. Army Research Office P.O. Box 12211 Research Triangle Park, North Carolina 27709 Attn: CRD-AA-IP	
Commander Naval Undersea Research & Development Center San Diego, California 92132 Attn: Technical Library, Code 133	1
Naval Weapons Center China Lake, California 93555 Attn: Head, Chemistry Division	1
Naval Civil Engineering Laboratory Port Hueneme, California 93041 Attn: Mr. W. S. Haynes	1
Professor O. Heinz Department of Physics & Chemistry Naval Postgraduate School Monterey, California 93940	
Dr. A. L. Slafkosky Scientific Advisor Commandant of the Marine Corps (Code RD-1) Washington, D.C. 20380	1

No. Copies

NASA-Lewis Research Center
21000 Brookpark Road
Cleveland, Ohio 44135
Attn: Dr. T. T. Serofini, MS-49-1 1

Dr. Charles H. Sherman, Code TD 121
Naval Underwater Systems Center
New London, Connecticut 1

Dr. William Risen
Department of Chemistry
Brown University
Providence, Rhode Island 02912 1

Dr. Alan Gent
Department of Physics
University of Akron
Akron, Ohio 44304 1

Mr. Robert W. Jones
Advanced Projects Manager
Hughes Aircraft Company
Mail Station D 132
Culver City, California 90230 1

Dr. C. Giori
IIT Research Institute
10 West 35 Street
Chicago, Illinois 60616 1

Dr. Jerome B. Lando 1
Dept. of Macromolecular Science
Case Western Reserve University
Cleveland, Ohio 44106

No. Copies

Dr. David Roylance
Department of Materials Science and Engineerir
Massachusetts Institute of Technology
Cambridge, Massachusetts 02039 1

Dr. W. A. Spitzig
United States Steel Corporation
Research Laboratory
Monroeville, Pennsylvania 15146 1

Dr. T. P. Conlon, Jr., Code 3622
Sandia Laboratories
Sandia Corporation
Albuquerque, New Mexico 87115 1

Dr. Martin Kaufmann, Head
Materials Research Branch, Code 4542
Naval Weapons Center
China Lake, California 93555 1

Dr. Charles Hicks
Naval Undersea Center
San Diego, California 92132 1

Mr. A. Johnson N43-12
National Highway Traffic Safety Admin. 1
2100 2nd Street, S.W.
Washington, D.C. 20590